molecules

MDPI

Article

The Chemical Constituents of Diaphragma Juglandis Fructus and Their Inhibitory Effect on α-Glucosidase Activity

Jinyan Tan [1,†], Yangang Cheng [1,2,†], Shihui Wang [1], Jianli Li [1], Haiqin Ren [1], Yuanbiao Qiao [2], Qingshan Li [2,*] and Yingli Wang [1,2,*]

[1] Shanxi Modern Chinese Medicine Engineering Laboratory, Shanxi University of Chinese Medicine, Jinzhong 030619, China; 15636833827@163.com (J.T.); chengyg1992@163.com (Y.C.); wangshihui9516@163.com (S.W.); lijianli1124ljl@163.com (J.L.); haiqinren@163.com (H.R.)

[2] Shanxi Key Laboratory of Innovative Drug for the Treatment of Serious Diseases Basing on the Chronic Inflammation, Shanxi University of Chinese Medicine, Jinzhong 030619, China; qiaoyb@sxtcm.edu.cn

* Correspondence: sxlqs0501@sxtcm.edu.cn (Q.L.); wyltyut@163.com (Y.W.); Tel.: +86-0351-3179901 (Y.W.)

† These authors contributed equally to this work.

Abstract: In our current investigation, 37 constituents (**1**–**37**), including 11 megastigmanes (**1**–**11**), 17 flavonoids (**12**–**28**) and 9 phenylpropanoids (**29**–**37**), were isolated from a 70%-EtOH extract of Diaphragma juglandis Fructus. Among them, compounds **1**–**3**, **12** and **29** were new compounds and their structures were elucidated on the basis of physicochemical evidence and meticulous spectroscopic analysis (NMR, HRESIMS and CD). Compounds **13**, **16**, **21** and **28** showed moderate inhibitory effect on α-glycosidase inhibitory activities, with IC_{50} values being in the range of 29.47–54.82 μM and stronger than the positive control (acarbose, 60.01 ± 4.82 μM).

Keywords: walnut; megastigmanes; bicyclic neomegastigmane; flavonoids; phenylpropanoids; α-glucosidase inhibition activity

check for updates

Citation: Tan, J.; Cheng, Y.; Wang, S.; Li, J.; Ren, H.; Qiao, Y.; Li, Q.; Wang, Y. The Chemical Constituents of Diaphragma Juglandis Fructus and Their Inhibitory Effect on α-Glucosidase Activity. *Molecules* **2022**, *27*, 3045. https://doi.org/10.3390/molecules27103045

Academic Editors: Bingyou Yang and Severina Pacifico

Received: 1 April 2022
Accepted: 3 May 2022
Published: 10 May 2022

1. Introduction

The walnut (*Juglans regia* L.) is consumed globally as a high economic value crop [1]. The edible portion of walnuts (kernel) has been processed into many types of foods due to its unique and highly nutritious nature and health-related benefits [2]. However, Diaphragma juglandis Fructus, the dry wooden diaphragm inside the walnut, mainly consists of undigestible fiber and lignin and is usually discarded as waste during the processing of the walnut [3]. In fact, Diaphragma juglandis Fructus is a traditional Chinese medicine and has been used to treat several illnesses such as insomnia, diarrhea, kidney deficiency and reproductive diseases for a long time [4,5]. It has also been used as an herbal tea and a dietary supplement in folk culture [6]. The research shows that Diaphragma juglandis Fructus is rich in a variety of bioactive components, such as flavonoids, saponins, phenolic acids and polysaccharides [7].

Previously, our team focused on the antidiabetic effect of Diaphragma juglandis Fructus, and it was found to improve symptoms of diabetes via the AKT/FoxO1 signaling pathway [8]. As part of our continuous program to identify new potential candidates to control diabetes using natural products, the subsequent phytochemical study led to the isolation of 37 constituents (**1**–**37**) from Diaphragma juglandis Fructus, including 11 megastigmanes (**1**–**11**) (Figure 1), (**12**–**28**) and **9** phenylpropanoids (**29**–**37**). Among them, compounds **1**–**3**, **12** and **29** were new compounds. Their structures were elucidated on the basis of physicochemical evidence, in-depth NMR spectroscopic analysis and high-resolution mass spectrometry. Meanwhile, the α-glucosidase inhibition activities of all isolates were evaluated. The isolation, structural identification and bioactivity evaluation of the obtained compounds are reported herein.

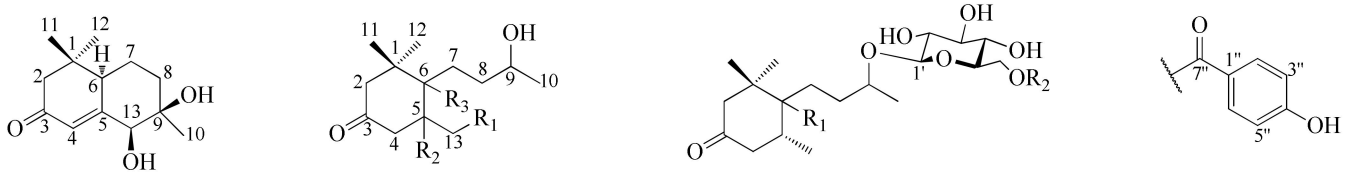

1

2 R_1=OH, R_2=H, R_3=OH, Δ^4, 6*S*
4 R_1=H, R_2=H, R_3=OH, Δ^4, 6*S*,9*R*
5 R_1=H, R_2=H, R_3=OH, Δ^4, Δ^7, 6*S*,9*R*
6 R_1=OH, R_2=H, R_3=H, Δ^4, 6*R*,9*R*
7 R_1=H, R_2=OH, R_3=OH, Δ^7, 5*S*,6*S*,9*R*

3 R_1=H, R_2=pOHBz, Δ^4, 6*R*,9*R*
8 R_1=H, R_2=H, 6*S*,9*R*
9 R_1=H, R_2=H, Δ^4, 6*S*,9*S*
10 R_1=H, R_2=H, Δ^4, 6*S*,9*R*
11 R_1=OH, R_2=pOHBz, Δ^4, Δ^7, 6*R*,9*S*

pOHBz

Figure 1. The structures of megastigmanes (**1**–**11**) isolated from Diaphragma juglandis Fructus.

2. Results and Discussion

2.1. Structural Elucidation

Compound **1** displayed a quasi-molecular ion peak at *m/z* 225.1489 ($[M+H]^+$, calcd 225.1490), in agreement with the molecular formula $C_{13}H_{20}O_3$, corresponding to four degrees of unsaturation. The analysis of ^{1}H-NMR data (Table 1) revealed that **1** possessed three methyls [δ_H 1.00, 1.03, 1.05 (3H each, both s, H_3-10, 11, 12)], three methylenes and a methine bearing an oxygen function [δ_H 4.08 (1H, d, J = 1.4 Hz, H-13)]. In addition, the ^{13}C-NMR (Figure S4) and DEPT spectra revealed a quaternary carbon bearing an oxygen function (δ_C 76.8), a trisubstituted olefin [δ_H 6.15 (1H, br s, H-4), δ_C 121.0 (C-4), 168.2 (C-5)] and a conjugated carbonyl carbon (δ_C 202.6). The planar structure of **1** was determined to be a bicyclic neomegastigmane skeleton through the interpretation of various NMR experiments [9], including HSQC, ^{1}H-^{1}H COSY and HMBC spectra. Namely, the ^{1}H-^{1}H COSY experiments of **1** indicated the presence of one partial written in red bold lines (Figure 2). In addition, obvious long-range correlations were observed between the following proton and carbon pairs in the HMBC experiments: H_2-2 and C-1, 3, 6; H-4 and C-5, 6, 13; H-6 and C-5; H_2-8 and C-6, 9, 13; H-13 and C-4, 5, 9, 10; H_3-10 and C-8, 9, 13; H_3-11 and C-1, 2, 6, 12; H_3-12; and C-1, 2, 6, 11 (blue arrow in Figure 2). Next, the relative stereostructure of **1** was clarified to be 9β-OH and 13β-OH by the NOESY experiment, in which correlations were observed between the following proton pairs: H_3-12 and H-6; H-6 and H-13; H-13; and H_3-10 (Figure 3). Based on the above-mentioned evidence, the structure of **1** was elucidated to be a bicyclic megastigmane named diamegastigmane A, as shown in Figure 1. Bicyclic megastigmanes are a small but growing group of natural products, and a possible biosynthetic pathway for **1** is further proposed in this paper (Figure 4).

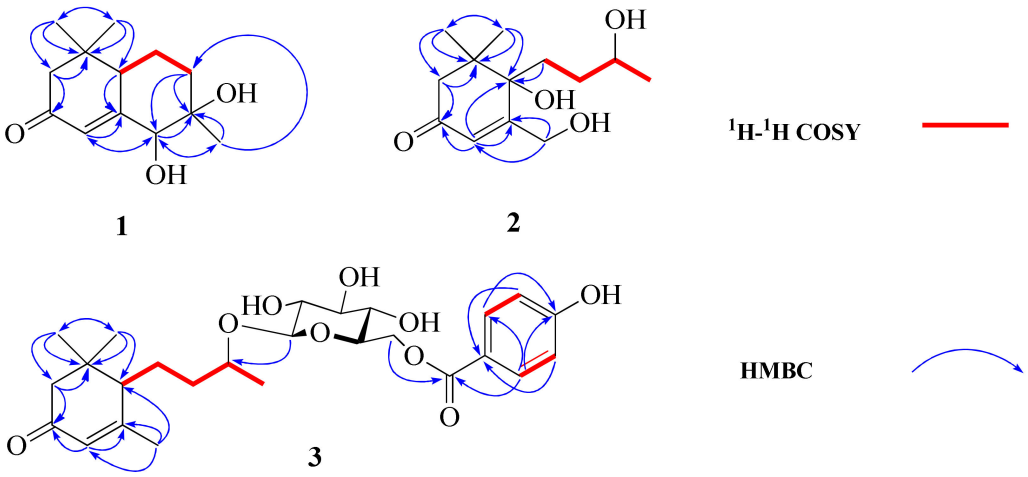

Figure 2. ^{1}H-^{1}H COSY and key HMBC correlations of compounds **1**–**3**.

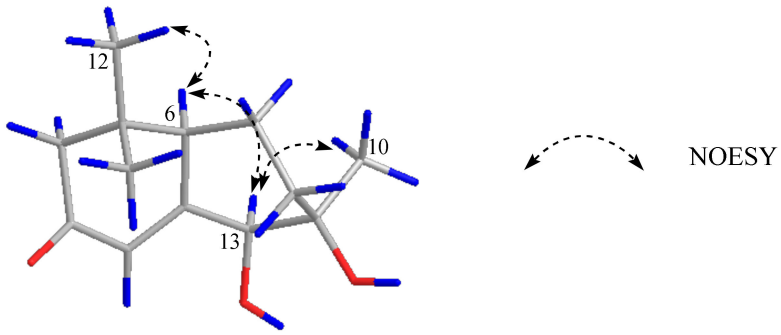

Figure 3. Key NOESY correlations of compound **1**.

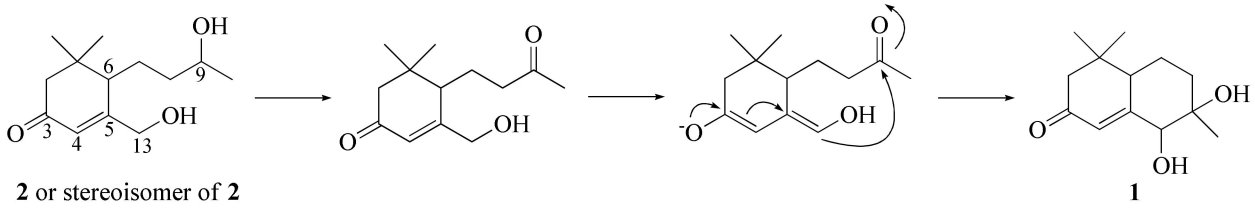

Figure 4. Plausible biogenetic pathway for compound **1**.

Table 1. ^{1}H-NMR (600 MHz, methanol-d_4) and ^{13}C-NMR (150 MHz, methanol-d_4) of compounds **1**–**3** (δ in ppm, J values in Hz).

Position	1		2		3	
	δ_H	δ_C	δ_H	δ_C	δ_H	δ_C
1	-	35.5	-	43.1	-	37.2
2	2.33 (d, 15.6) 2.13 (d, 15.6)	50.4	2.61 (d, 18.3) 2.20 (d, 18.3)	50.8	2.34 (d, 17.3) 1.87 (d, 17.3)	48.1
3	-	202.6	-	200.9	-	202.3
4	6.15 (br. s)	121.0	6.10 (br. s)	122.4	5.70 (br. s)	125.3
5	-	168.2	-	173.9	-	169.9
6	2.16 (dd, 12.9, 4.5)	49.2	-	78.8	1.81 (t, 5.2)	52.2
7	1.94 (m) 1.39 (dd, 13.4, 4.0)	25.3	1.98 (m) 1.78 (m)	35.8	1.92 (m) 1.35 (m)	26.8
8	1.86 (ddd, 13.4, 3.7, 3.0) 1.72 (td, 13.4, 4.3)	39.1	1.67 (m) 1.43 (m)	34.9	2.19 (m) 1.55 (m)	37.6
9	-	76.8	3.67 (m)	68.9	3.73 (m)	76.5
10	1.03 (s)	19.3	1.16 (d, 6.2)	23.5	1.17 (d, 6.2)	20.4
11	1.00 (s)	25.8	1.09 (s)	24.4	0.90 (s)	28.9
12	1.05 (s)	28.7	1.04 (s)	23.5	0.96 (s)	27.4
13	4.08 (d, 1.4)	80.2	4.39 (t, 1.9)	63.1	1.90 (d, 1.1)	24.8
1′					4.34 (d, 7.7)	102.8
2′					3.17 (m)	75.2
3′					3.39 (m)	78.0
4′					3.39 (m)	72.0
5′					3.58 (m)	75.2
6′					4.56 (dd, 11.8, 2.3) 4.42 (dd, 11.8, 6.4)	64.9
1						
″					-	122.3
2″, 6″					7.89 (d, 8.8)	132.9
3″, 5″					6.83 (d, 8.8)	116.2
4″					-	163.7
7″					-	167.9

"m" means multiplet or overlapped with other signals.

Compound **2** was assigned a molecular formula of $C_{13}H_{22}O_4$ through an analysis of the HRESIMS ion peak at *m/z* 485.3115 ([2M+H]$^+$, calcd 485.3114). The ^{1}H-NMR (Table 1) spectrum showed the presence of two methyl singlets [δ_H 1.04, 1.09 (3H each, both s, H_3-11, 12)], a doublet methyl singlet [δ_H 1.16 (3H, d, J = 6.2 Hz, H_3-10)], a methine and methylene bearing a hydroxyl group [δ_H 3.67 (1H, m, H-9), 4.39 (2H, t, J = 1.9 Hz, H_2-13)] and a trisubstituted olefin [δ_H 6.10 (1H, br. s, H-4)]. The ^{13}C-NMR spectrum exhibited 13 carbon signals. In combination with the HSQC spectrum, carbon signals were identified as three methyls [δ_C 23.5 (C-10), 24.4 (C-11), 23.5 (C-12)], four methylenes [δ_C 50.8 (C-2), 35.8 (C-7), 34.9 (C-8), 63.1 (C-13)], an oxygenated methine carbon [δ_C 68.9 (C-9)], a quaternary carbon [δ_C 43.1 (C-1)], an oxygenated quaternary carbon [δ_C 78.8 (C-6)], two olefinic carbons [δ_C 122.4 (C-4), 173.9 (C-5)] and a carbonyl carbon [δ_C 200.9 (C-3)]. The NMR spectroscopic data (Table 1) for **2** closely resembled those of apocynol B, and further analysis of the 2D NMR spectra revealed that the significant difference was the absence of one olefin in the side chain [10]. The ^{1}H-^{1}H COSY spectrum of **2** enabled the identification of the H_2-7/H_2-8/H-9/H_3-10 unit. Further, HMBC correlations from H_2-7 to C-1, C-5 and C-6 arranged the carbon chain that connected to C-6 (Figure 2). Moreover, the CD spectrum indicated a 6*S*-configuration due to a positive Cotton effect at 323 nm and a negative Cotton effect at 272 nm [11]. However, the chirality of C-9 in the side chain was difficult to assign due to the lack of direct evidence and thus, needs to be further determined. Consequently, the structure of **2** was identified (Figure 1) and named diamegastigmane B.

Compound **3** has a molecular formula of $C_{26}H_{36}O_9$ based on the HRESIMS ion at *m/z* 493.2442 ([M+H]$^+$, calcd 493.2437). The ^{1}H-NMR spectrum (Table 1) of **3** showed two doublet signals at δ_H 7.89 (2H, d, J = 8.8 Hz, H-2″,6″) and 6.83 (2H, d, J = 8.8 Hz, H-3″,5″), attributed to the AA′BB′ system in a 1,4-substituted benzene ring, assigned to the 4-hydroxybenzoyl group. The location of the 4-hydroxybenzoyl group was established at C-6′ in the pyranosyl moiety according to the long-range correlation from a proton signal at δ_H 4.34 (1H, d, J = 7.7 Hz, H-1′) to a carbon signal at δ_C 167.9 (C-7″) in the HMBC spectrum (Figure 2).

The 1D NMR spectroscopic data (Table 1) of 3 showed significant similarity to those of hirtionoside C, except for the replacement of the gallic acid at the 6′-position by a 4-hydroxybenzoic acid [12]. The absolute configuration at the 6-position was confirmed to be *R* by the CD spectrum (positive Cotton effect at 333 nm) [13], and those at the 9-position were also determined to be *R* by comparing ^{13}C NMR data according to the *β*-D-glycosylation-induced shift-trend rule [14]. Therefore, the structure of **3** was determined (Figure 1) and named diamegastigmane C.

Compound **12** was obtained as yellow amorphous powder (Figure 5). Its molecular formula was deduced as $C_{14}H_{14}O_9$ on the basis of a quasi-molecular ion peak in HRESIMS ($C_{14}H_{15}O_9$, *m/z* 327.0715 [M+H]$^+$, calcd 327.0716). The ^{1}H-NMR spectrum of **12** (Table 2) displayed two meta-coupled aromatic protons at δ_H 6.20 (1H, d, J = 2.1 Hz, H-6) and 6.31 (1H, d, J = 2.1 Hz, H-8), together with a singlet at δ_H 8.09 (1H, s, H-2) in the low field. The ^{13}C-NMR spectrum (Table 2) showed 14 carbon signals, including 9 aromatic carbon signals and 5 sugar carbon signals. The 1D NMR spectra data of **12** showed a similar pattern to those of 3,5,7-trihydroxylchromone-3-*O*-*α*-L-arabinopyranoside, except for the sugar part [15]. The anomeric carbon of 12 at δ_C 109.5 (C-1′) and other four sugar carbon signals at δ_C 83.3 (C-2′), 78.7 (C-3′), 87.2 (C-4′) and 62.9 (C-5′) were similar to those of *α*-L-arabinofuranose in juglanin [16]. In addition, the structure of the sugar part in 12 was further confirmed to be L-arabinofuranose after derivatization and comparison with an authentic sample in a GC analysis. Based on the above evidence and the 2D NMR spectra (Figure 6), the structure of **12** was elucidated to be 3,5,7-trihydroxylchromone-3-*O*-*α*-L-arabinofuranoside.

Table 2. ^{1}H-NMR (600 MHz, methanol-d_4) and ^{13}C-NMR (150 MHz, methanol-d_4) of compound **12**. (δ in ppm, J values in Hz).

Position	δH	δC	Position	δH	δC
2	8.09 (s)	148.7	9	-	159.3
3	-	140.0	10	1.03 (s)	106.4
4	-	179.0	1′	5.48 (s)	109.5
5	-	163.4	2′	4.31 (dd, 3.2, 1.1)	83.3
6	6.20 (dd, 2.1)	100.0	3′	3.94 (dd, 5.9, 3.2)	78.7
7	-	166.1	4′	4.13 (m)	87.2
8	6.31 (d, 2.1)	95.0	5′	3.78 (dd, 12.1, 3.4) 3.67 (dd, 12.1, 5.6)	62.9

"m" means multiplet or overlapped with other signals.

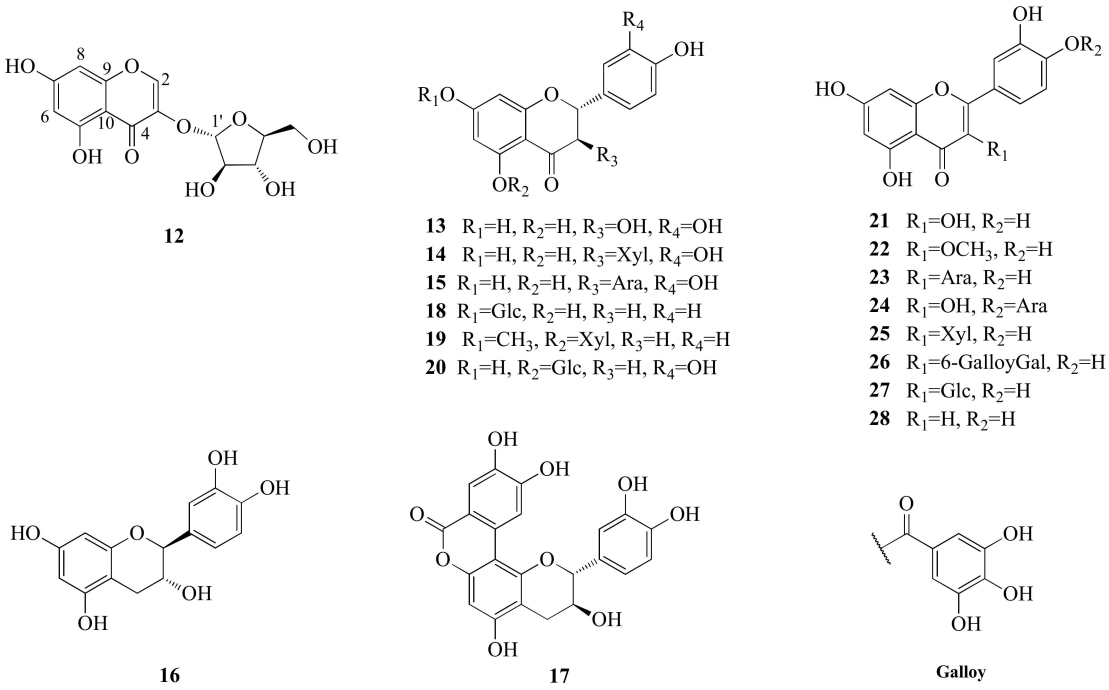

Figure 5. The structures of flavonoids (**12**–**28**) isolated from Diaphragma juglandis Fructus. (Ara = α-L-arabinofuranose; Xyl = β-D-xylopyranose; Glc = β-D-glucopyranose; Gal = β-D-galactopyranose).

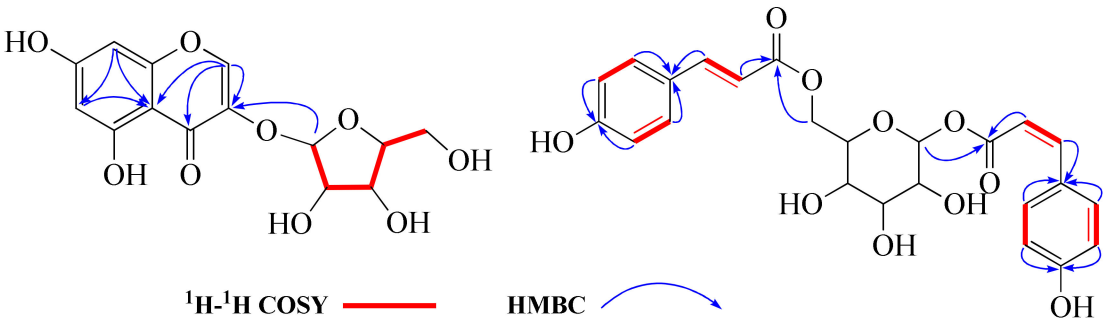

Figure 6. ^{1}H-^{1}H COSY and key HMBC correlations of compounds **12** and **29**.

Compound **29**, a yellow amorphous powder (Figure 7), had a molecular formula of $C_{24}H_{24}O_{10}$ based on HRESIMS at m/z 471.1286 $[M-H]^-$ (calcd for 471.1290) and corresponding to 13 degrees of unsaturation. A comparison of the ^{1}H- and ^{13}C-NMR spectroscopic data of **29** (Table 3) with those of 1,6-di-*O*-(*E*)-coumaroyl-β-D-glucopyranoside (**30**) suggested that these two compounds were closely related in structure [17], while the variations

mainly occurred in the vicinity of C-7″ and C-8″ [C-3″/5″ ($\Delta\delta_C$ −1.1), C-4″ (−1.3), C-9″ (−2.8), C-2″/6″ (+ 2.8) and C-8″ (+ 0.5)], indicating that 29 was the C-7″/C-8″ *cis-trans* isomerization of 30. The structure of 29 was further confirmed by analysis of coupling constants ($J_{C\text{-}7''} = J_{C\text{-}8''}$ = 12.8 Hz in **29** and $J_{C\text{-}7''} = J_{C\text{-}8''}$ = 15.9 Hz in **30**) and the 2D NMR spectra (Figure 6). Accordingly, the structure of **29** was characterized as 1-*O*-(*Z*)-coumaroyl,6-*O*-(*E*)-coumaroyl-*β*-D-glucopyranoside.

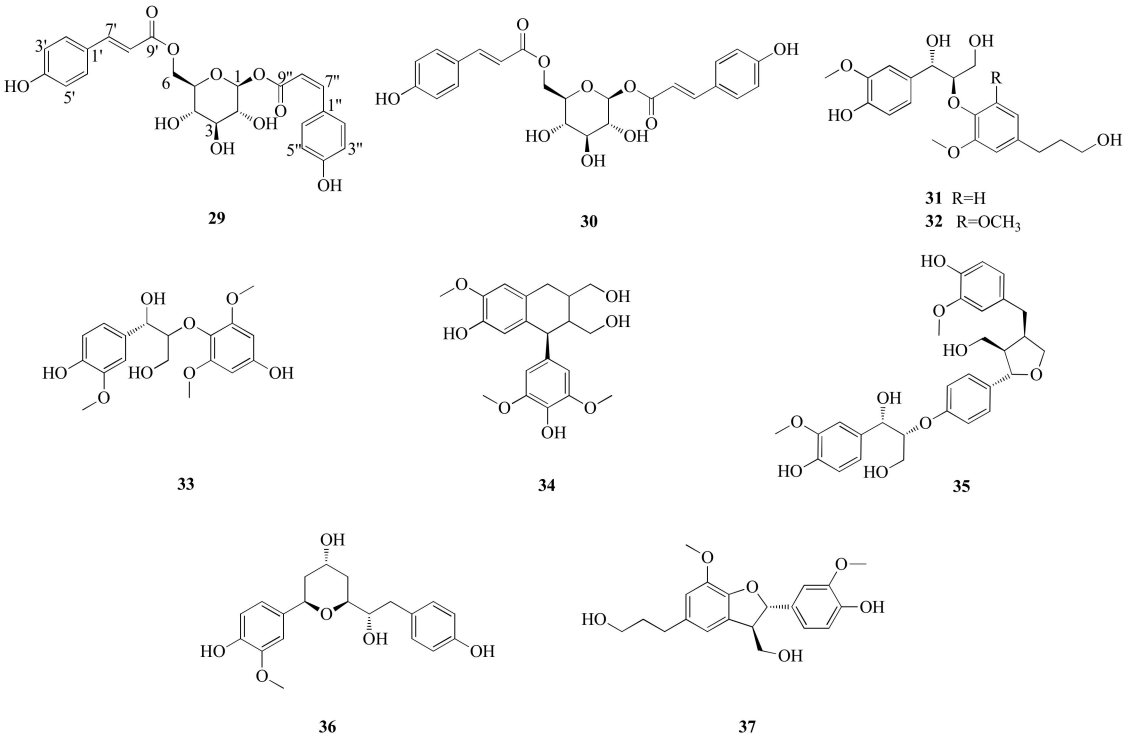

Figure 7. The structures of phenylpropanoids (**29**–**37**) isolated from Diaphragma juglandis Fructus.

Table 3. ^{1}H-NMR (600 MHz) and ^{13}C-NMR (150 MHz) of **29** in methanol-d_4 (δ in ppm, J values in Hz).

Position	δH	δC	Position	δH	δC
1	5.57 (d, 8.2)	95.5	7′	7.64 (d, 15.9)	146.9
2	3.39 (m)	73.9	8′	6.37 (d, 15.9)	114.9
3	3.48 (m)	77.9	9′	-	169.1
4	3.42 (m)	71.3	1″	-	127.4
5	3.67 (m)	76.3	2″,6″	7.71 (d, 8.7)	134.1
6	4.52 (dd, 12.0, 1.9) 4.32 (dd, 12.0, 5.5)	64.4	3″,5″	6.75 (d, 8.7)	115.9
1′	-	127.2	4″	-	160.4
2′,6′	7.45 (d, 8.6)	131.2	7″	6.95 (d, 12.8)	147.0
3′,5′	6.79 (d, 8.6)	116.8	8″	5.83 (d, 12.8)	115.4
4′	-	161.3	9″	-	166.5

"m" means multiplet or overlapped with other signals.

In addition, 8 known megastigmanes (blumenol B (**4**) [18], vomifoliol (**5**) [19], aglycone of euodionoside G (**6**) [20], bridelionol C (**7**) [21], myrsinionoside A (**8**) [22], byzantionoside B (**9**) [23], blumenol C glucoside (**10**) [23] and (6*R*, 9*S*)-6′-(4″-hydroxybenzoyl)-roseoside (**11**) [24]); 16 known flavonoids, including 5 flavanonols (taxifolin (**13**) [25] and derivatives {taxifolin-3-*β*-D-xylopyranoside (**14**) [26], taxifolin-3-*O*-*α*-L-arabinofuranoside (**15**) [27]}, (+)-catechin (**16**) [28] and derivative {catechin lactone A (**17**) [29]}), 3 flavanones (naringenin derivatives {naringenin 7-*O*-*β*-D-glucopyranoside (**18**) [30]}, eriodictyol derivatives {sakuranetin 5-*O*-*β*-D xylopyranoside (**19**) [30] and (2*R*)-eriodictyol-5-*O*-*β*-D-glucoside

(**20**) [31]}), 7 flavonols (quercetin (**21**) [32] and derivatives {3-*O*-methylquercetin (**22**) [33], avicularin (**23**) [34], quercetin-3-*O*-*α*-D-arabinofuranoside (**24**) [34], quercetin 3-*O*-*β*-D-xylopyranoside (**25**) [35], quercetin-3-*O*-(6″-*O*-galloyl)-*β*-D-galactopyranoside (**26**) [36] and quercetin-3-*O*-*β*-D-glucopyranoside (**27**) [37]}) and 1 flavone (luteolin (**28**) [38]); and 8 known phenylpropanoids, including 1 phenylpropionic acid (1,6-di-*O*-(*E*)-coumaroyl-*β*-D-glucopyranoside (**30**) [17]), 3 phenylpropanols (erythro-(7*S*,8*R*)-guaiacyl-glycerol-*β*-*O*-4′-dihydroconiferyl ether (**31**) [39], 1-(4′-hydroxy-3′-methoxyphenyl)-2-[4″-(3-hydroxypropyl)-2″,6″-dimethoxyphenoxy]propane-1,3-diol (**32**) [40] and rosalaevin B (**33**) [41]), 1 cyclolignan (5-methoxy-(+)-isolariciresinol (**34**) [42]), 2 monoepoxylignans (erythro-guaiacyl-glycerol-*β*-*O*-4′-(5′)-methoxylariciresinol (**35**) [43] and rhoiptelol B (**36**) [44] and 1 benzofuran lignan (dihydrodehydodiconiferyl alcohol (**37**) [45]), were isolated from Diaphragma juglandis Fructus and their structures were determined based on the spectroscopic data and the literature (Figures 1, 5 and 7).

2.2. Glucosidase Inhibitory Assay

Alpha-glucosidase is an enzyme that hydrolyzes the carbohydrates to monosaccharides in the final step of carbohydrate digestion. Therefore, inhibiting the activity of *α*-glucosidase can effectively inhibit sugar uptake, thereby achieving lowered blood sugar [46]. Diaphragma juglandis Fructus was found to improve symptoms of diabetes [8] and the total flavonoids from it showed significant *α*-glucosidase inhibitory activities [47]. In order to search for bioactive substances to treat type 2 diabetes using Diaphragma juglandis Fructus, all isolated constituents (**1**–**37**) were assessed for antidiabetic activity using an in vitro *α*-glycosidase inhibition assay. As shown in Table 4, compounds **13, 16, 21** and **28** exhibited much more potent activity with the IC_{50} values of 40.39, 54.82, 29.47 and 35.41 μM being lower than the positive control, acarbose (60.01 μM). However, the IC_{50} values of other compounds were either over the positive control or inactive for *α*-glycosidase inhibition at 100 μM.

Table 4. *α*-Glucosidase inhibitory activity of compounds **1**–**37**.

Compound	IC_{50} (μM)	Compound	IC_{50} (μM)
1–11	>100	**22**	67.74 ± 6.41
12	92.35 ± 7.24	**23–25,27**	>100
13	40.39 ± 4.14	**26**	77.15 ± 12.36
14	95.78 ± 12.62	**28**	35.41 ± 3.87
15, 17–20	>100	**29–34,36,37**	>100
16	54.82 ± 7.47	**35**	87.74 ± 13.41
21	29.47 ± 2.95	**Acarbose**	60.01 ± 4.82

Data expressed as mean ± SD (n = 3).

Most of the bioactive compounds were flavonoids, suggesting that flavonoids might be the main bioactive substances contributing to the *α*-glucosidase inhibitory activity of Diaphragma juglandis Fructus. Furthermore, the structures of the A, B and C rings in the flavonoids were closely related to the inhibitory activity. Consistent with the previous reports, comparison among quercetin (**21**) and luteolin (**28**) revealed that hydroxylation at the 3-position of flavone enhanced the inhibitory effect. Comparison among (+)-catechin (**16**), quercetin (**21**) and luteolin (**28**) suggested the saturation of the 2,3-double bond in the C ring seemed to decrease the inhibitory activity [48]. In addition, among the taxifolin (**13**) and derivatives (**14, 15**), taxifolin showed the strongest inhibitory effect, indicating that the presence of a sugar moiety at C-3 may be responsible for the lowered activity [49]. In addition, galloyl moieties strengthen the inhibitory effects of flavonoids against the *α*-glucosidase (such as compound **26**) [50].

3. Materials and Methods

3.1. General Experimental Procedures

Optical rotations were determined by a Jasco P-2000 digital polarimeter. CD spectra were recorded on a Bio-Logic MOS-450 spectropolarimeter. One-dimensional (1D) and two-dimensional (2D) NMR spectra were measured on a Bruker 600 spectrometer. HRESIMS data were obtained using a Q Exactive Focus LC-MS/MS spectrometer (Thermo Fisher, MA, USA) or Triple TOF™ 5600 MS/MS system from Applied AB Sciex (Foster City, CA, USA). Medium-pressure liquid chromatography was performed with Buchi C610. To perform the preparative HPLC separation, a C_{18} preparative HPLC colum (21.2 mm × 250 mm, 5 μm, Sharpsil-U C18) on a Shimadzu LC-16P instrument equipped with an RID-20A refractive index detector was used for purification. Silica gel (200–300 mesh, Qingdao Marine Chemical Ltd., Qingdao, China) and RP-18 reversed-phase silica gel (YMC Company Ltd., Tokyo, Japan) were used for column chromatography. All organic solvents were analytical grade (Tianjin zhiyuan Chemical Regents Co., Ltd., Tianjin, China).

The α-glucosidase was obtained from Sigma-Aldrich (Shanghai) Trading Co., Ltd (Shanghai, China). p-nitrophenyl-α-D-glucopyranoside was obtained from Macklin Co., Ltd. (Lot# C12592180, Shanghai, China). Acarbose was purchased from bayer Co., Ltd. (Lot# BJ59027, Beijing, China).

3.2. Plant Material

Diaphragma juglandis Fructus was purchased from Anguo Chinese medicinal materials markets (Hebei Province) in March 2021 and identified by Professor Xiang-ping Pei (Shanxi University of Chinese Medicine). A voucher specimen (No. 20210301) was deposited at Shanxi Modern Chinese Medicine Engineering laboratory (Shanxi University of Chinese Medicine).

3.3. Extraction and Isolation

Diaphragma juglandis Fructus (5 kg) was extracted with 70% EtOH (40 L × 3) and dried under reduced pressure to afford 1.1 kg of crude extract. This extract was then suspended in H_2O and partitioned sequentially with petroleum ether (82 g), EtOAc (280 g) and *n*-butyl alcohol (416 g). The EtOAc partition (260 g) was then fractionated on a silica gel column (CH_2Cl_2-MeOH, 50:0, 50:1, 30:1, 15:1, 10:1, 5:1, 3:1, 2:1, 1:1, 0:1, *v*/*v*) to yield 8 fractions (A-H). Of these, fraction B (15.3 g) was chromatographed on an ODS column (MeOH-H_2O, 10–100% MeOH) to yield 15 subfractions (B1-B15). Subfraction B3 was subjected to purification over a preparative HPLC to afford compounds **4** (2.5 mg, t_R = 16.5 min) and **5** (3.7 mg, t_R = 16.7 min). B4 was further purified by a preparative HPLC to obtain compounds **13** (4.2 mg, t_R = 16.8 min) and **34** (1.6 mg, t_R = 15.6 min). Then, B5 was also purified using a preparative HPLC to give compounds **1** (3.1 mg, t_R = 18.9 min), **6** (2.6 mg, t_R = 18.8 min), **31** (2.7 mg, t_R = 16.5 min) and **32** (6.5 mg, t_R = 16.9 min). B7 was separated by a preparative HPLC to create compounds **33** (6.5 mg, t_R = 18.3 min) and **36** (3.9 mg, t_R = 17.8 min). B8 was purified by a preparative HPLC to yield compounds **35** (12.1 mg, t_R = 19.8 min) and **37** (32.3 mg, t_R = 19.2 min). B9 was applied to a preparative HPLC to give compounds **29** (5.2 mg, t_R = 20.5 min) and **30** (12.8 mg, t_R = 20.1 min). B11 was purified with a preparative HPLC to yield compounds **19** (4.2 mg, t_R = 22.2 min), **20** (5.3 mg, t_R = 23.1 min) and **21** (2.1 mg, t_R = 23.3 min). Fraction C (20.7 g) was then eluted on an ODS column to yield 13 subfractions (C1-C13). One of these subfractions, C2, was further purified on a preparative HPLC. As a result, crops of compounds **2** (2.9 mg, t_R = 13.5 min), **7** (1.4 mg, t_R = 14.0 min), **12** (15.8 mg, t_R = 14.8 min) and **27** (8.0 mg, t_R = 11.5 min) were obtained. Two other subfractions (C8 and C10) were further applied to a preparative HPLC to afford compounds **8** (6.3 mg, t_R = 20.9 min) and **3** (2.8 mg, t_R = 22.9 min). On the other hand, fraction D (10.8 g) was eluted on an ODS column (MeOH-H_2O, 10–100% MeOH) to obtain 12 subfractions (D1-D12). Subfraction D6 was purified using a preparative HPLC to give compounds **9** (9.0 mg, t_R = 19.9 min), **10** (13.9 mg, t_R = 20.0 min), **11** (10.8 mg, t_R = 19.5 min), **15** (5.1 mg, t_R = 18.8 min), **22** (20.6 mg,

t_R = 19.2 min) and **23** (2.9 mg, t_R = 19.6 min). Fraction E (13.5 g) was separated on an ODS column (MeOH-H_2O, 10–100% MeOH) to obtain 10 subfractions (E1-E10). Subfraction E7 was purified using a preparative HPLC to yield compounds **14** (8.2 mg, t_R = 16.0 min) and **18** (23.9 mg, t_R = 17.9 min). Then, fraction F (18.5 g) was chromatographed on an ODS column (MeOH-H_2O, 10–100% MeOH) to give 11 subfractions (F1-F11), and F7 was separated on a preparative HPLC. As a result, compounds **16** (10.1 mg, t_R = 16.3 min), **17** (7.5 mg, t_R = 16.8 min), **25** (21.6 mg, t_R = 17.5 min) and **26** (7.5 mg, t_R = 18.6 min) were obtained. F8 was purified with a preparative HPLC to obtain compounds **24** (11.8 mg, t_R = 19.0 min) and **28** (2.8 mg, t_R = 18.7 min).

3.4. Characterization of Compounds **1**–**3**, **12**, **29**

Diamegastigmane A (**1**): white amorphous powder; $[\alpha]_D^{20}$ = +11 (c = 0.1, MeOH); HRESIMS *m/z* 225.1489 $[M+H]^+$ (calcd. for $C_{13}H_{21}O_3$, *m/z* 225.1490); ^{1}H-NMR (methanol-d_4, 600 MHz) and ^{13}C-NMR (methanol-d_4, 150 MHz), see Table 1.

Diamegastigmane B (**2**): white amorphous powder; $[\alpha]_D^{20}$ = +10 (c = 0.1, MeOH); HRESIMS *m/z* 485.3115 $[2M+H]^+$ (calcd. for $C_{26}H_{45}O_8$, *m/z* 485.3114); ^{1}H-NMR (methanol-d_4, 600 MHz) and ^{13}C-NMR (methanol-d_4, 150 MHz), see Table 1.

Diamegastigmane C (**3**): white amorphous powder; $[\alpha]_D^{20}$ = +35 (c = 0.1, MeOH); HRESIMS *m/z* 493.2442 $[M+H]^+$ (calcd. for $C_{26}H_{37}O_9$, *m/z* 493.2437); ^{1}H-NMR (methanol-d_4, 600 MHz) and ^{13}C-NMR (methanol-d_4, 150 MHz), see Table 1.

3,5,7-trihydroxylchromone-3-*O*-*α*-L-arabinofuranoside (**12**): yellow amorphous powder; $[\alpha]_D^{20}$ = -166 (c = 0.1, MeOH); HRESIMS *m/z* 327.0715 $[M+H]^+$ (calcd. for $C_{14}H_{15}O_9$, *m/z* 327.0716); ^{1}H-NMR (methanol-d_4, 600 MHz) and ^{13}C-NMR (methanol-d_4, 150 MHz), see Table 2.

1-*O*-(*Z*)-coumaroyl,6-*O*-(*E*)-coumaroyl-*β*-D-glucopyranoside (**29**): Yellow amorphous powder; $[\alpha]_D^{24}$ = -50 (c = 0.3, MeOH); HRESIMS *m/z* 471.1286 $[M-H]^-$ (calcd. for $C_{24}H_{23}O_{10}$, *m/z* 471.1290); ^{1}H-NMR (methanol-d_4, 600 MHz) and ^{13}C-NMR (methanol-d_4, 150 MHz), see Table 3.

3.5. Acid Hydrolysis of Compounds **3**, **12** *and* **29**

In order to determine the absolute configuration of monosaccharides in the new compounds, the acid hydrolysis of compounds **3**, **12** and **29** were performed according to the previous literature [51]. The *n*-hexane fractions were then detected by GC-MS with a DB-5 capillary column, and the absolute configuration of sugar components was confirmed to be D-glucose, L-arabinofuranose and D-glucose in compounds **3**, **12** and **29**, respectively, compared with standards.

3.6. α-Glucosidase Inhibitory Assay

The α-glucosidase inhibition assay was performed according to a previous report [52] with a slight difference: the concentration of α-glucosidase was diluted to 0.15 unit/mL. The volume of α-glucosidase added to the 96-well plate was 10 μL. Acarbose was used as the positive control.

4. Conclusions

In summary, a detailed phytochemical investigation on the EtOAc partition of 70% ethanol extract of Diaphragma juglandis Fructus was carried out to afford 37 constituents in this research, and five of them were new structures (**1**–**3**, **12**, **29**). Their structures were elucidated based on MS and NMR spectroscopic data and comparison with data reported in the literature. Compounds **1**–**3** were new megastigmanes. Among them, compound **1** was a bicyclic neomegastigmane, and a plausible biogenetic pathway for it was further discussed in this paper. Compound **12** was a new chromone with α-L-arabinofuranoside. Compound **29** was a new phenylpropanoid. The α-glucosidase inhibition activity was also investigated. Compounds **13**, **16**, **21** and **28** were found to be quite potent and most of them were flavonoids, suggesting that flavonoids might be the main bioactive substances

contributing to the α-glucosidase inhibitory activity of Diaphragma juglandis Fructus. These findings also revealed that these compounds could be target compounds for the development of new antidiabetic agents.

Supplementary Materials: The following supporting information can be downloaded at: https://www.mdpi.com/article/10.3390/molecules27103045/s1. A scheme of extraction and isolation (Figure S1), spectroscopic data for compounds **1**–**3**, **12** and **29** (Figures S2–S39), ^{13}C-NMR spectra of compounds **4**–**11**, **13**–**28**, **30**–**37** (Figures S40–S71) are available as Supporting Information.

Author Contributions: J.T. and Y.C. carried out the extraction and purification process. S.W. and J.L. performed the whole experiment process as assistants. H.R. contributed to the revision of the paper. Y.Q. assisted with the α-glucosidase inhibitory assay. Q.L. contributed to the elucidation of the chemical structures. Y.W. designed the whole research plan and wrote the paper. All authors have read and agreed to the published version of the manuscript.

Funding: This research was funded by the "1331 Project" Quality and Efficiency Improvement Construction Plan Project ((2021) No. 4); Shanxi Provincial Health Commission (2020094); Open Fund of the Shanxi Key Laboratory of Innovative Drugs for the Treatment of Serious Diseases Based on Chronic Inflammation, Shanxi University of Chinese Medicine (2021sxcxyw10).

Institutional Review Board Statement: Not applicable.

Informed Consent Statement: Not applicable.

Data Availability Statement: Not applicable.

Acknowledgments: We thank the academic assistance of the Shanxi Leader Team of Medical Science & Technology Innovations (Grant: 2020TD02).

Conflicts of Interest: The authors declare no conflict of interest.

Sample Availability: Samples of all the isolated compounds are available from the authors.

References

1. Hu, Q.; Liu, J.; Li, J.; Liu, H.; Dong, N.; Geng, Y.Y.; Lu, Y.; Wang, Y. Phenolic composition and nutritional attributes of diaphragma juglandis fructus and shell of walnut (*Juglans regia* L.). *Food Sci. Biotechnol.* **2019**, *29*, 187–196. [CrossRef] [PubMed]
2. Liu, R.; Zhao, Z.; Dai, S.; Che, X.; Liu, W. Identification and quantification of bioactive compounds in Diaphragma juglandis Fructus by UHPLC-Q-Orbitrap HRMS and UHPLC-MS/MS. *J. Agric. Food Chem.* **2019**, *67*, 3811–3825. [CrossRef] [PubMed]
3. Zhang, Y.G.; Kan, H.; Chen, S.X.; Thakur, K.; Wang, S.; Zhang, J.G.; Shang, Y.F.; Wei, Z.J. Comparison of phenolic compounds extracted from Diaphragma juglandis fructus, walnut pellicle, and flowers of *Juglans regia* using methanol, ultrasonic wave, and enzyme assisted-extraction. *Food Chem.* **2020**, *321*, 126672. [CrossRef]
4. Zhao, H.; Bai, H.; Jing, Y.; Li, W.; Yin, S.; Zhou, H. A pair of taxifolin-3-*O*-arabinofuranoside isomers from *Juglans regia* L. *Nat. Prod. Res.* **2017**, *31*, 945–950. [CrossRef] [PubMed]
5. Meng, Q.; Li, Y.; Xiao, T.; Zhang, L.; Xu, D. Antioxidant and antibacterial activities of polysaccharides isolated and purified from Diaphragma juglandis fructus. *Int. J. Biol. Macromol.* **2017**, *105*, 431–437. [CrossRef] [PubMed]
6. Meng, Q.; Wang, Y.; Chen, F.; Xiao, T.; Zhang, L. Polysaccharides from Diaphragma juglandis fructus: Extraction optimization, antitumor, and immune-enhancement effects. *Int. J. Biol. Macromol.* **2018**, *115*, 835–845. [CrossRef]
7. Wang, D.; Mu, Y.; Dong, H.; Yan, H.; Hao, C.; Wang, X.; Zhang, L. Chemical constituents of the ethyl acetate extract from Diaphragma juglandis Fructus and their inhibitory activity on nitric oxide production in vitro. *Molecules* **2017**, *23*, 72. [CrossRef]
8. Li, G.Y.; Cheng, Y.G.; Zeng, T.C.; Li, M.J.; Sun, R.R.; Li, H.F.; Kong, X.P.; Pei, M.R. Action mechanism of total flavonoids of Diaphragma Juglandis Fructus in treating type 2 diabetes mellitus based on network pharmacology and cellular experimental validation of AKT/FoxO1 signaling pathway. *Drug Eval. Res.* **2019**, *42*, 30–40.
9. Muraoka, O.; Morikawa, T.; Zhang, Y.; Ninomiya, K.; Nakamura, S.; Matsuda, H.; Yoshikawa, M. Novel megastigmanes with lipid accumulation inhibitory and lipid metabolism-promoting activities in HepG2 cells from Sedum sarmentosum. *Tetrahedron* **2009**, *65*, 4142–4148. [CrossRef]
10. Kanchanapoom, T.; Sirikatitham, A.; Otsuka, H.; Ruchirawat, S. A new megastigmane diglycoside from *Erythroxylum cuneatum* Blume. *J. Asian Nat. Prod. Res.* **2006**, *8*, 747–751. [CrossRef]
11. Matsunami, K.; Otsuka, H.; Takeda, Y.; Miyase, T. Reinvestigation of the absolute stereochemistry of megastigmane glucoside, icariside B(5). *Chem. Pharm. Bull.* **2010**, *58*, 1399–1402. [CrossRef] [PubMed]
12. Nomoto, Y.; Sugimoto, S.; Matsunami, K.; Otsuka, H. Hirtionosides A–C, gallates of megastigmane glucosides, 3-hydroxyoctanoic acid glucosides and a phenylpropanoid glucoside from the whole plants of Euphorbia hirta. *J. Nat. Med.* **2013**, *67*, 350–358. [CrossRef] [PubMed]

13. Yan, J.K.; Shi, X.L.; Donkor, P.O.; Zhu, H.J.; Gao, X.M.; Ding, L.Q.; Qiu, F. Nine pairs of megastigmane enantiomers from the leaves of *Eucommia ulmoides* Oliver. *J. Nat. Med.* **2017**, *71*, 780–790. [CrossRef] [PubMed]
14. Matsunami, K.; Ousuka, H.; Takeda, Y. Structural revisions of blumenol C glucoside and byzantionoside B. *Chem. Pharm. Bull.* **2010**, *58*, 438–441. [CrossRef]
15. Chen, G.; Jin, H.Z.; Li, X.F.; Zhang, Q.; Shen, Y.H.; Yan, S.K.; Zhang, W.D. A new chromone glycoside from *Rhododendron spinuliferum*. *Arch. Pharm. Res.* **2008**, *31*, 970–972. [CrossRef]
16. Kim, H.J.; Woo, E.R.; Park, H. A novel lignan and flavonoids from *Polygonum aviculare*. *J. Nat. Prod.* **1994**, *57*, 581–586. [CrossRef]
17. Madikizela, B.; Aderogba, M.A.; Finnie, J.F.; Van Staden, J. Isolation and characterization of antimicrobial compounds from *Terminalia phanerophlebia* Engl. & Diels leaf extracts. *J. Ethnopharmacol.* **2014**, *156*, 228–234.
18. Shi, L.L.; Ma, G.X.; Yang, J.S.; Gulinar, S.; Jia, X.G. Chemical constituents from plant of *Stelleropsis tianschanica*. *Chin. Tradit. Herb. Drugs* **2016**, *47*, 223–226.
19. Yang, J.Q.; He, W.J.; Tan, H.N.; Chu, H.B.; Zhang, Y.M.; Mei, W.L.; Dai, H.F. Chemical constituents of *Pedicularis cephalantha* Franch and *P. siphonantha* Don. *Nat. Prod. Res. Dev.* **2009**, *21*, 600–603.
20. Yamamoto, M.; Akita, T.; Koyama, Y.; Sueyoshi, E.; Matsunami, K.; Otsuka, H.; Shinzato, T.; Takashima, A.; Aramoto, M.; Takeda, Y. Euodionosides A-G: Megastigmane glucosides from leaves of *Euodia meliaefolia*. *Phytochemistry* **2008**, *69*, 1586–1596. [CrossRef]
21. Sueyoshi, E.; Liu, H.; Matsunami, K.; Otsuka, H.; Shinzato, T.; Aramoto, M.; Takeda, Y. Bridelionosides A–F: Megastigmane glucosides from *Bridelia glauca* f. balansae. *Phytochemistry* **2006**, *67*, 2483–2493. [CrossRef] [PubMed]
22. Otsuka, H.; Zhong, X.N.; Hirata, E.; Shinzato, T.; Takeda, Y. Myrsinionosides A-E: Megastigmane glycosides from the leaves of *Myrsine seguinii* Lev. *Chem. Pharm. Bull.* **2001**, *49*, 1093–1097. [CrossRef] [PubMed]
23. Takeda, Y.; Zhang, H.J.; Masuda, T.; Honda, G.; Otsuka, H.; Sezik, E.; Yesilada, E.; Sun, H.D. Megastigmane glucosides from *Stachys byzantine*. *Phytochemistry* **1997**, *44*, 1335–1337. [CrossRef]
24. Bermúdez, J.; Rodríguez, M.; Hasegawa, M.; González-Mujica, F.; Duque, S.; Ito, Y. (6*R*,9*S*)-6″-(4″-hydroxybenzoyl)-roseoside, a new megastigmane derivative from *Ouratea polyantha* and its effect on hepatic glucose-6-phosphatase. *Nat. Prod. Commun.* **2012**, *7*, 973–976. [CrossRef] [PubMed]
25. Agrawal, P.K.; Agarwal, S.K.; Rastogi, R.P.; Osterdahal, B.G. Dihydroflavanonols from *Cedrus deodara*, A (13)C NMR study. *Planta Medica* **1981**, *43*, 82–85. [CrossRef]
26. Yao, F.Y.; Huang, D.D.; Huang, G.H.; Xue, D.; Sun, L.N. Chemical constituents of *Illicium brevistylum*. *Chin. Tradit. Herb. Drugs* **2014**, *45*, 1536–1539.
27. Liu, Y.; Rong, X.H.; Tan, J.Y.; Pan, J.; Guan, W.; Kuang, H.X.; Yang, B.Y. Chemical constituents of flavonoids and alkaloids from leaves of *Datura metel*. *Chin. Tradit. Herb. Drugs* **2021**, *52*, 4141–4152.
28. Zhao, J.; Zhou, X.W.; Chen, X.B.; Wang, Q.X. α-Glucosidase inhibitory constituents from *Toona sinensis*. *Chem. Nat. Compd.* **2009**, *45*, 244–246. [CrossRef]
29. Hong, S.S.; Suh, H.J.; Oh, J.S. Phenolic chemical constituents of the stem barks of *Robinia pseudoacacia*. *Chem. Nat. Compd.* **2017**, *53*, 359–361. [CrossRef]
30. Qi, J.J.; Yan, Y.M.; Wang, C.X.; Cheng, Y.X. Compounds from *Lycium ruthenicum*. *Nat. Prod. Res. Dev.* **2018**, *30*, 345–353.
31. Pan, J.Y.; Zhou, Y.; Zou, K.; Wu, J.; Li, Q.X.; Zhang, S. Chemical constituents of *Balanophora involucrate*. *Chin. Tradit. Herb. Drugs* **2008**, *39*, 327–331.
32. Li, Y.L.; Li, K.M.; Su, M.X.; Leung, K.T.; Cheng, Y.W.; Zhang, Y.W. Studies on antiviral constituents in stems and leaves of *Pithecellibium clypearia*. *China J. Chin. Mater. Med.* **2006**, *31*, 397–400.
33. Mu, L.H.; Zhang, D.M. Studies on chemical constituents of *Cercis chinensis*. *China J. Chin. Mater. Med.* **2006**, *31*, 1795–1797.
34. Chen, G.; Jin, H.Z.; Li, X.F.; Zhang, Q.; Shen, Y.H.; Yan, S.K.; Zhang, W.D. Chemical constituents from *Rhododendron spinu-liferum*. *Chem. Nat. Compd.* **2009**, *45*, 725–727. [CrossRef]
35. Park, B.J.; Matsuta, T.; Kanazawa, T.; Park, C.H.; Chang, K.J.; Onjo, M. Phenolic compounds from the leaves of *Psidium guajava* II. Quercetin and its glycosides. *Chem. Nat. Compd.* **2012**, *48*, 477–479. [CrossRef]
36. Masuda, T.; Iritani, K.; Yonemori, S.; Oyama, Y.; Takeda, Y. Isolation and antioxidant activity of galloyl flavonol glycosides from the seashore plant, *Pemphis acidula*. *Biosci. Biotechnol. Biochem.* **2001**, *65*, 1302–1309. [CrossRef]
37. Wang, Q.; Xu, D.R.; Shi, X.H.; Qin, M.J. Flavones from *Potentilla discolor* Bunge. *Chin. J. Nat. Med.* **2009**, *7*, 361–364. [CrossRef]
38. Ma, X.Q.; Zheng, C.J.; Zhang, Y.; Hu, C.L.; Lin, B.; Fu, X.Y.; Han, L.Y.; Xu, L.S.; Rahman, K.; Qin, L.P. Antiosteoporotic flavonoids from *Podocarpium poducarpum*. *Phytochem. Lett.* **2013**, *6*, 118–122. [CrossRef]
39. Huang, X.X.; Zhou, C.C.; Li, L.Z.; Li, F.F.; Lou, L.L.; Li, D.M.; Ikejima, T.; Peng, Y.; Song, S.J. The cytotoxicity of 8-*O*-4′ neolignans from the seeds of *Crataegus pinnatifida*. *Bioorg. Med. Chem. Lett.* **2013**, *23*, 5599–5604. [CrossRef]
40. Gao, L.; Tian, H.; Lv, P.J.; Wang, J.P.; Wang, Y.F. Chemical constituents of *Sapium sebiferum* leaves. *China J. Chin. Mater. Med.* **2015**, *40*, 1518–1522.
41. Li, X.; Cao, W.; Shen, Y.; Li, N.; Dong, X.P.; Wang, K.J.; Cheng, Y.X. Antioxidant compounds from *Rosa laevigata* fruits. *Food Chem.* **2012**, *130*, 575–580. [CrossRef]
42. Su, J.S.; Qin, F.Y.; Zhang, Y.; Cheng, Y.X. Compounds of Codonopsis pilosula. *J. Chin. Med. Mater.* **2018**, *41*, 863–867.
43. Han, H.Y.; Liu, H.W.; Wang, N.L.; Yao, X.S. Sequilignans and dilignans from *Campylotropis hirtella* (Franch.) Schindl. *Nat. Prod. Res.* **2008**, *22*, 990–995. [CrossRef]

44. Jiang, Z.H.; Tanaka, T.; Hirata, H.; Fukuoka, R.; Kouno, I. Three diarylheptanoids from *Rhoiptelea chiliantha*. *Phytochemistry* **1996**, *43*, 1049–1054. [CrossRef]
45. Fang, J.M.; Lee, C.K.; Cheng, Y.S. Lignans from leaves of *Juniperus chinensis*. *Phytochemistry* **1992**, *31*, 3659–3661.
46. Hu, G.L.; Peng, X.R.; Dong, D.; Nian, Y.; Gao, Y.; Wang, X.Y.; Hong, D.F.; Qiu, M.H. New ent-kaurane diterpenes from the roasted arabica coffee beans and molecular docking to α-glucosidase. *Food Chem.* **2021**, *345*, 128823. [CrossRef] [PubMed]
47. Cheng, Y.G.; Li, G.Y.; Tan, J.Y.; Liu, Y.; Li, H.F.; Yao, Y.J.; Zhang, J.Y.; Yang, B.Y.; Pei, M.R. Antioxidant of total favonoids from Diaphragma Juglandis Fructus. and its inhibitory effects on α-glucosidase and α-amylase activity in vitro. *J. Liaoning Univ. TCM* **2018**, *20*, 22–25.
48. Tadera, K.; Minami, Y.; Takamatsu, K.; Matsuoka, T. Inhibition of α-glucosidase and α-amylase by flavonoids. *J. Nutr. Sci. Vitaminol.* **2006**, *52*, 149–153. [CrossRef]
49. Jani, N.A.; Sirat, H.M.; Ahmad, F.; Aminudin, N.I. New sesquiterpene dilactone and β-carboline alkaloid and the α-glucosidase inhibitory activity of selected phytochemicals from *Neolitsea cassia* (L.) Kosterm. *Nat. Prod. Res*. 2021. Available online: https://www.tandfonline.com/doi/full/10.1080/14786419.2021.1961134 (accessed on 30 March 2022).
50. Zhu, J.Z.; Chen, C.; Zhang, B.; Huang, Q. The inhibitory effects of flavonoids on α-amylase and α-glucosidase. *Crit. Rev. Food Sci. Nutr.* **2020**, *60*, 695–708. [CrossRef]
51. Tan, J.Y.; Liu, Y.; Cheng, Y.G.; Sun, Y.P.; Pan, J.; Guan, W.; Li, X.M.; Huang, J.; Jiang, P.; Guo, S.; et al. New withanolides with anti-inflammatory activity from the leaves of *Datura metel* L. *Bioorg. Chem.* **2020**, *95*, 103541. [CrossRef]
52. Peng, C.Y.; Lu, J.; Liu, J.Q.; Huang, H.L.; Zhu, Y.Y.; Shu, J.C. Three novel pterosin dimers form *Pteris obtusiloba*. *Fitoterapia* **2020**, *146*, 104713. [CrossRef] [PubMed]